Russian Journal of General Chemistry, Vol. 71, No. 4, 2001, pp. 519–524. Translated from Zhurnal Obshchei Khimii, Vol. 71, No. 4, 2001, pp. 558–564.

P(IV)–P(V) Coordinational Isomerism of Phosphorus *N*-α-Haloethylimines

E. A. Romanenko

Institute of Bioorganic and Petroleum Chemistry, National Academy of Sciences of Ukraine, Kiev, Ukraine

Received July 5, 1999

Abstract — The semiempirical MNDO–PM3 method in supramolecular approximation was used to study the structure of (*N*-α-haloethylimino)chloro(*o*-phenylenedioxy)phosphoranes $R^1{}_3CR^2X–N–P(Cl)O_2C_6H_2(R^3\text{-}m)_2$, where R^1 = H, Cl, F, $R^2 = R^3$ = H, Cl, and X = F, Cl, Br, and of their 1 : 2 solvates with chloroform, as well as alternative mechanisms of the P(IV)–P(V) holotropic rearrangement. It was found that the activation barrier of the sigmatropic rearrangement increases in the order Br < Cl < F, in parallel with increasing thermodynamic stability of a more stable phosphorane isomer with an axial–equatorial arrangement of the dioxaphosphole ring. It was shown that the most favorable pathway of the phosphorus–carbon halotropic rearrangement of a phosphorus *N*-α-haloethylimine, both nonsolvated and solvated with two molecules of chloroform, is the sigmatropic transformation.

Previously we considered the P(III)–P(IV) coordinational isomerism of a *P*-chloroylide [1] and the P(V)–P(VI) isomerism of amidinium halophosphorates [2]. A missing link in the general picture of halotropic interconversions of the main classes of high-coordination organophosphorus compounds there remained a P(IV)–P(V) halotropism which was recently experimentally observed in the phosphazochloroethane–chlorophosphorane system [3].

Here we present the results of quantum-chemical calculations by the MNDO–PM3 method [4] in supramolecular approximation of the structure of (*N*-α-haloethylimino)chloro(*o*-phenylenedioxy)phosphoranes $R^1_3CCR^2X–N{=}P(Cl)O_2C_6H_2(R^3\text{-}m)_2$, where R^1 = H, Cl, F, $R^2 = R^3$ = H, Cl, and X= F, Cl, Br, and of their 1 : 2 solvates, as well as of altenative mechanisms of the P,C-halotropic transformation in the PNC triad, accompanied by the P(IV)–P(V) coordinational isomerization. The calculation results were compared with the experimental ^{35}Cl NQR data [5]. Calculations with full geometry optimization were performed for structures $M \cdot n HCCl_3$, where n = 0, 2 , and M is *P*-chloroimine **Ia**–**VIa**, intermediate **Ib**–**VIb**, halophosphorane **Id**–**VId**, or transition state **Ic**–**VIc** of the sigmatropic 1,3-halogen shift according to scheme (1):

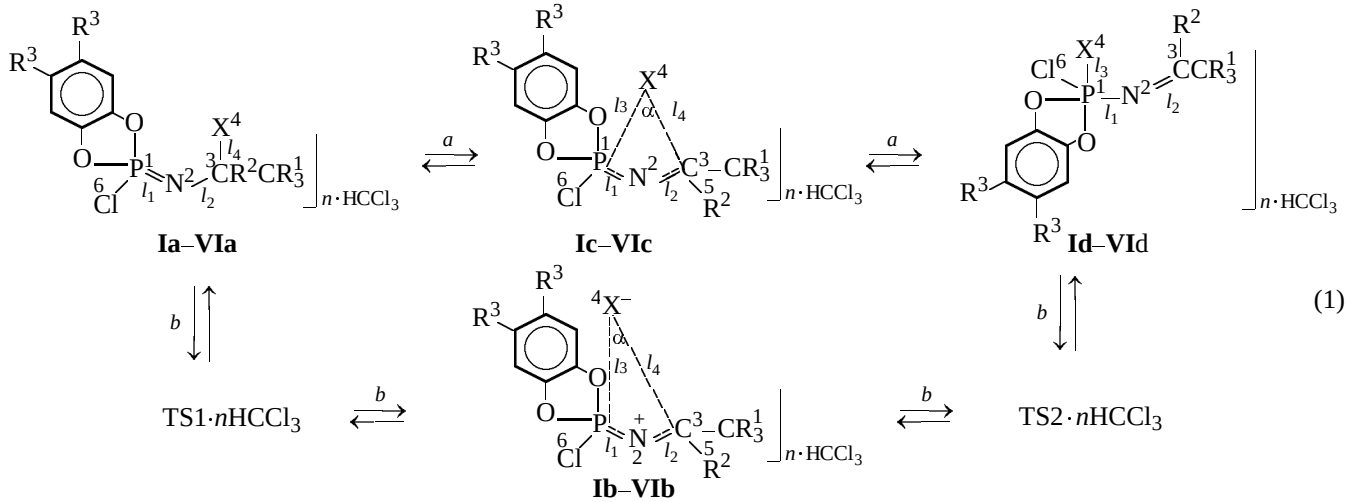

(1)

$R^1 = R^2$ = Cl, R^3 = H, X = F (**Ia**–**Id**), Cl (**IIa**–**IId**), Br (**IIIa**–**IIId**); $R^1 = R^2 = R^3$ = Cl, X = Cl (**IVa**–**IVd**); $R^1 = R^2$ = R^3 = H, X = Cl (**Va**–**Vd**); R^1 = F, R^2 = Cl, R^3 = H, X = Cl (**VIa**–**VId**).

1070-3632/01/7104-0519 $25.00

Table 1. Main energetic and geometric parameters of *P*-chloroimines **Ia**–**VIa**, intermediates (IM) **Ib**–**VIb**, halophosphoranes **Id**–**VId**, and transition states (TS) **Ic**–**VIc** of the sigmatropic mechanism of the 1,3-halogen shift, calculated by the MNDO–PM3 method

Structure	ΔH_{f298}, kJ/mol	l_1, Å	l_2, Å	l_3, Å	l_4, Å	α, deg	τ[a], deg	ν_{im}, cm^{-1}
Ia	–674.5	1.594	1.426	–	1.361	112.5[b]	55.6	–
IM **Ib**	–349.3	1.707	1.286	7.213	8.909	16.2	1.9	–
TS **Ic**	–501.8	1.684	1.352	1.903	1.790	87.0	14.8	776
Id	–702.5	1.751	1.272	1.512	–	119.1[c]	35.9	–
IIa	–507.8	1.594	1.414	–	1.809	114.3[b]	64.2	–
IM **IIb**	–272.8	1.701	1.291	7.420	8.728	17.9	4.9	–
TS **IIc**	–442.8	1.669	1.343	2.416	2.199	69.3	22.9	365
IId	–557.6	1.746	1.277	2.131	–	92.2[c]	22.0	–
IIIa	–475.2	1.603	1.393	–	1.977	112.3[b]	68.6	–
IM **IIIb**	–256.5	1.699	1.289	7.358	9.040	15.9	7.1	–
TS **IIIc**	–432.3	1.652	1.349	2.679	2.276	63.8	22.8	262
IIId	–517.6	1.725	1.285	2.340	–	88.1[c]	25.1	–
IVa	–555.7	1.595	1.416	–	1.809	114.4[b]	57.6	–
IM **IVb**	–263.9	1.698	1.292	8.590	9.829	15.8	3.4	–
TS **IVc**	–489.0	1.667	1.344	2.412	2.200	69.4	22.4	366
IVd	–606.0	1.743	1.278	2.129	–	92.8[c]	22.7	–
Va	–455.6	1.587	1.433	–	1.847	109.7[b]	91.6	–
IM **Vb**	–249.2	1.698	1.295	7.417	8.437	18.2	4.8	–
TS **Vc**	–418.9	1.653	1.362	2.473	2.154	67.0	28.7	320
Vd	–529.2	1.729	1.289	2.153	–	94.6	22.4	–
VIa	–1093.9	1.600	1.408	–	1.798	115.3[b]	63.0	–
IM **VIb**	–835.4	1.708	1.284	7.421	8.948	16.8	1.0	–
TS **VIc**	–1013.8	1.677	1.332	2.409	2.205	69.5	22.9	394
VId	–1131.6	1.749	1.272	2.135	–	91.8[c]	22.9	–

[a] Dihedral angle $X^4P^1N^2C^3$. [b] Bond angle $X^4C^3N^2$. [c] Bond angle $X^4P^1N^2$.

The calculation results are presented in Tables 1–4. The mutual location of the substrate and chloroform molecules for solvates $M \cdot 2HCCl_3$ are given in scheme (2) as graphic representations of optimized *Z* matrices. The corresponding geometric parameters are given in Table 1.

According to the calculations, *P*-chloroimines **Ia**–**VIa** and their phosphorane isomers **Id**–**VId** are thermodynamically stable compounds, the latter being more stable. The consecutive substitution of fluorine by chlorine and bromine in the series **IIa, IIIa** and **Id, IId, IIId** results in a considerable shortening of the neighboring bonds C^3–N^2 and P^1–N^2 in both isomers (Table 1). The PNCC entity in imines **Ia**–**VIa** has a *transoid* structure with the phosphorus–oxygen bonds of the dioxaphosphole ring eclipsing the dichloromethylene group, which is confirmed by the close ^{35}Cl NQR frequencies of the latter at 37.399 and 37.306 MHz [5]. The increased ionicity (0.17 units, as evaluated from the average frequency 37.35 MHz and a known equation [6]) and C^3–Cl^4 bond length (1.766–1.847 Å) favor the subsequent 1,3 shift of the α-chlorine atom. The phosphorus tetrahedron is slightly distorted (the Cl^6PN and OPN angles in isomer **IIa** are 114 and 120°, respectively) due to the decreased OPO angle (96.6°–97.7°) in the five-membered heterocycle, while the trigonal geometry of the nitrogen atom is distorted due to the opening of the PNC angle to 125.9–133.9°. Along with the P=N bond length (Table 1), the latter two values do not go beyond the ranges 154–164 Å and 120–137° corresponding to experimental values of the P=N bond and the PNC angle in phosphorus imines [7, 8].

For chlorotropic isomer **IId**, the calculations give three phosphorane structures [scheme (3)] with close energies of formation, kJ/mol: *gauche* (–536.1), *anti* (–554.5), and *syn* (–557.6). Hence, all the three structures are thermodynamically more stable than imine **IIa** (Table 1). The least stable *gauche* isomer has two axial P–Cl bonds (2.12 Å) and the C^3–Cl^5 bond in the

Table 2. Atomic charges (q_i, *e*), atomic coefficients (c_{ij}), and energies (ε_i, eV)[a] of frontier orbitals of *P*-chloroimines **Ia**–**VIa**, intermediates (IM) **Ib**–**VIb**, halophosphoranes **Id**–**VId**, and transition states (TS) **Ic**–**VIc** of the sigmatropic mechanism of the 1,3-halogen shift, calculated by the MNDO–PM3 method

Atom, parameter	q_i	c_{ij}		q_i	c_{ij}		q_i	c_{ij}		q_i	c_{ij}	
		HOMO	LUMO		HOMO	LUMO		HOMO	LUMO		HOMO	LUMO
		Ia			IM **Ib**			TS **Ic**			**Id**	
P^1	1.91	0.04	–0.54	1.92	0.09	–0.54	2.00	0.00	0.49	2.07	–0.02	–0.58
C^3	0.24	–0.02	0.12	0.05	–0.01	0.11	0.27	–0.01	–0.32	0.04	0.01	0.13
F^4	–0.14	0.00	–0.02	–0.36	0.08	0.01	–0.46	0.03	0.27	–0.32	0.01	–0.14
ε_i		–9.77	–2.06		–7.13	–3.72		–9.56	–2.19		–9.30	–1.99
		IIa			IM **IIb**			TS **IIc**			**IId**	
P^1	1.90	0.05	0.54	1.95	0.03	–0.55	2.02	0.00	0.48	2.01	0.00	–0.57
C^3	0.11	–0.03	–0.12	0.06	0.00	0.10	0.24	–0.01	–0.35	0.04	–0.01	0.09
Cl^4	–0.06	0.00	–0.01	–0.80	–0.39	–0.02	–0.58	0.04	0.29	–0.52	–0.03	0.00
ε_i		–9.76	–2.11		–7.09	–4.22		–9.70	–2.50		–9.46	–2.49
		(–9.88)	(–2.28)		(–8.15)	(–4.49)		(–9.91)	(–2.72)		(–9.66)	(–2.79)
		IIIa			IM **IIIb**			TS **IIIc**			**IIId**	
P^1	1.90	–0.04	0.54	1.95	0.03	–0.55	1.96	0.03	–0.50	1.97	0.00	–0.56
C^3	0.13	0.02	0.13	0.06	0.00	0.11	0.22	–0.05	0.30	0.02	0.03	0.09
Br^4	–0.20	–0.02	0.01	–0.85	0.61	0.03	–0.62	–0.27	–0.23	–0.66	–0.01	–0.28
ε_i		–9.83	–2.23		–7.15	–4.26		–9.50	–2.47		–9.65	–2.57
		(–9.97)	(–2.44)		(–8.26)	(–4.52)		(–9.88)	(–2.72)		(–9.85)	(–2.84)
		IVa			IM **IVb**			TS **IVc**			**IVd**	
P^1	1.89	0.02	–0.54	1.95	–0.01	–0.55	2.02	0.00	–0.48	2.01	0.00	–0.57
C^3	0.10	–0.01	0.12	0.06	0.00	0.10	0.24	–0.01	0.34	0.04	0.01	0.09
Cl^4	–0.06	0.00	–0.01	–0.88	–0.89	0.01	–0.57	0.02	–0.29	–0.51	0.02	0.00
ε_i		–9.47	–2.26		–7.09	–4.44		–9.37	–2.65		–9.21	–2.65
		Va			IM **Vb**			TS **Vc**			**Vd**	
P^1	1.85	–0.06	–0.52	1.91	0.02	–0.54	1.98	0.01	–0.53	1.97	–0.01	–0.56
C^3	0.15	0.04	0.10	0.20	0.00	0.10	0.33	0.00	0.23	0.13	0.00	0.06
Cl^4	–0.18	0.03	–0.02	–0.81	–0.37	–0.01	–0.60	–0.03	–0.21	–0.56	–0.03	0.01
ε_i		–9.55	–1.76		–7.02	–3.93		–9.51	–1.85		–9.24	–2.14
		VIa			IM **VIb**			TS **VIc**			**VId**	
P^1	1.90	–0.04	–0.54	1.96	0.04	–0.55	2.03	0.00	–0.48	2.01	0.01	0.57
C^3	0.35	0.02	0.13	0.00	–0.01	0.10	0.18	–0.01	0.35	–0.01	–0.01	–0.09
Cl^4	–0.04	0.01	–0.01	–0.79	–0.47	–0.03	–0.57	0.04	–0.29	–0.52	–0.03	0.00
ε_i		–9.88	–2.26		–7.18	–4.45		–9.84	–2.75		–9.59	–2.68

[a] The energies of frontier orbitals for solvates $M \cdot 2HCCl_3$ are given in parentheses.

gauche position to them. The stability increases by 18 kJ/mol in going to the permutational *anti* isomer in which the first axial position is still occupied by the chlorine atom *anti* to the C^3–Cl^5 bond, while the second one is occupied by an axial–equatorial oxygen atom of the diazaphosphole ring. The change of the C^3–Cl^5 bond to the *syn* position with respect the axial P–Cl^4 bond gives the most stable *syn* isomer **IId** whose structure is in complete agreement with the six signals in the ^{35}Cl NQR spectrum (77 K) [5] at 25.804 (P-Cl^a), 30.590 (P–Cl^e), 35.674 (C_{sp^2}–Cl) 39.933, 40.464, and 41.025 MHz (C_{sp^3}–Cl), corresponding to the axial and equatorial positions of the chlorine atom of the trigonal phosphorus bipyramid and of the chlorine atoms of the =CCl and CCl_3 groups (cf. the trigonal-bipyramidal environment of

Table 3. Main energetic and geometric characteristics of solvated *P*-chloroimines **IIa$_2$, IIIa**$_2$, intermediates (IM) **IIb$_2$**, **IIb$_2$**, halophosphoranes **IId$_2$**, **IIId$_2$**, and transition states (TS) **IIb$_2$**, **IIIc$_2$** of the 1,3-halogen for solvates M · 2HCCl$_3$, calculated by the MNDO–PM3 method

Structure	ΔH_{f298}, kJ/mol	M = **IIa–IId, IIIa–IIId**						HCCl$_3$, Δl(C–H), Å	l(E···HCCl$_3$)[b], Å
		l_1, Å	l_2, Å	l_3, Å	l_4, Å	α, deg	τ[a], deg		
					n = 2				
IIa$_2$	–693.7	1.596	1.410	–	1.811	115.0[c]	58.0	0.006	2.786 (Cl)
								0.006	2.572 (Cl)
IM **IIb$_2$**	–557.3	1.698	1.290	7.575	9.306	15.2	1.5	0.081	1.735 (Cl[4])
								0.080	1.735 (Cl[4])
TS **IIc$_2$**[d]	–639.6	1.658	1.345	2.530	2.189	67.6	23.7	0.007	2.413 (Cl[4])
								0.007	2.443 (Cl[4])
IId$_2$	–751.2	1.737	1.280	2.140	–	92.9[e]	22.0	0.006	2.461 (Cl[4])
								0.005	2.494 (Cl[6])
					n = 2				
IIIa$_2$	–665.5	1.601	1.385	–	1.976	115.2[b]	55.8	0.005	2.569 (Cl)
								0.008	2.643 (Cl)
IM **IIIb$_2$**	–492.6	1.697	1.291	7.652	9.378	15.0	1.5	0.049	1.850 (Br[4])
								0.050	1.851 (Br[4])
TS **IIIc$_2$**[d]	–635.5	1.645	1.344	2.875	2.273	61.3	29.5	0.005	2.600 (Br[4])
								0.006	2.606 (Br[4])
IIId$_2$	–712.5	1.719	1.287	2.352	–	88.5[e]	25.0	0.005	2.608 (Br[4])
								0.004	2.554 (Cl[6])

[a] Dihedral angle $X^4P^1N^2C^3$. [b] The shortest intermolecular contact: the E atom is given in parentheses; and for solvates **IIa$_2$, IIIa$_2$** the contacts relate to chlorine atoms of the trichloromethyl group. [c] Bond angle $X^4Cu^3N^2$. [d] ν_{im} = 311 and 234 cm^{-1} for TS **IIc$_2$** and TS **IIIc$_2$**, respectively. [e] Bond angle $X^4P^1N^2$.

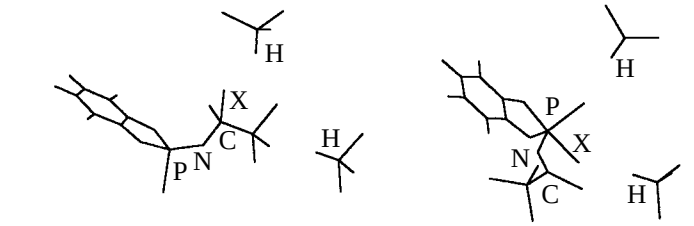

IIa$_2$, IIIa$_2$ **IId$_2$, IIId$_2$** (2)

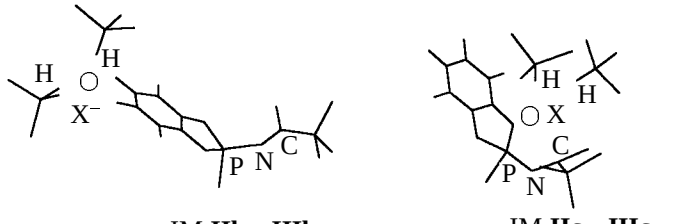

IM **IIb$_2$, IIIb$_2$** IM **IIc$_2$, IIIc$_2$**

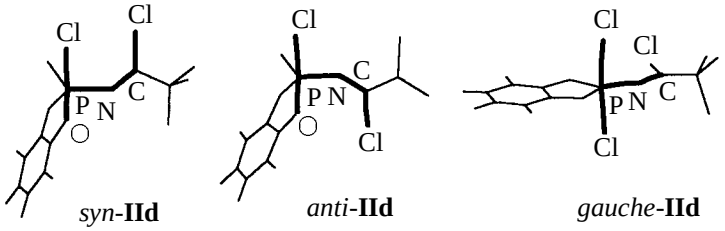

syn-**IId** *anti*-**IId** *gauche*-**IId** (3)

the phosphorus atom in 1,3,2λ^5-diazaphosphetidine [9]). *Syn* isomer **IId** is characterized by the maximum difference between the axial (2.131 Å) and equatorial (2.065 Å) PCl bond lengths, as well as between the axial (1.746 Å) and equatorial (1.714 Å) dioxaphosphole phosphorus–oxygen bond lengths, as well as a considerable decrease of the OPO angle (to 92.7°). The deviation from a strictly *syn* arrangement of the P–X^a and C^3–R^2 bonds in compounds **Id**–**VId** is 23°–33°. In phosphorane isomers **Id** and **IIId**, the bulkier halogen atoms (Cl and Br, respectively) are expelled to the less sterically hindered axial position inspite of the higher electronegativity of fluorine in the first case. The solvating chloroform molecules reside near the trichloromethyl group in isomers **IIa, IIIa** and the PCl(Br) bonds in isomers **IId, IIId** [see scheme (2) in which for clarity we showed the PNC triad, "transit" halogen atom, and chloroform hydrogen atoms], thus producing minimial changes in the geometry (Table 1) and the solvation energy (11 and 19 kJ/mol for the starting imine **IIa** and phosphorane **IId**, respectively).

Transition states **Ic**–**VIc** for the 1,3-halogen shift by sigmatropic pathway *a* of the imine $\rightleftarrows$ phosphorane isomerization is a four-membered heterocycle with intermediate P–N and N–C bond lengths, practically equalized bonds of the P^{1}Cl^{4}C^3 triad, and the angle α equal to 64–87° (Table 1). The displacement of the halogen atom X^4 in the course of isomerization of phosphoranes **Id**–**VId** occurs from the apical position (equatorial for the fluorine atom) of the weakest P–Hlg^a bond, but in the transition state this halogen atom still occupies the same position but with another *transoid* partner, Cl^6, which is more electronegative than the oxygen atom [scheme (1)]. This fact points to a low activation barrier for the permutational isomerization of the trigonal phosphorus bipyramid in the phosphoranes under study (cf. [3]), along with above-noted low heat of permutational transformation for phosphorane **IId**. After the departure of the halogen, the equatorial environment of phosphorus and the environment of the C^3 atom undergo pyramidalization to ΣP(C^3)~354°, accompanied by displacement of atoms in the bases of the P and C^3 pyramids, to and away from to the transition halogen atom X^4. In the series of transition states **Ic**–**IIIc**, the dependence from the principal quantum number of halogen shows up in a gradual increase of the P^1(C^3)···X^4 distances to 2.3–2.7 Å as the angle α decreases to 63.8°. Therewith, the shapes of the transition vectors for transition states **Ic**–**VIc** prove similar to each other and corresponding to a shift of X^4, parallel to a line connecting the P^1 and C^3 atoms, while their imaginary fundamental frequencies strongly decrease in the series of transition states **Ic**–**IIIc** and much weaker decrease with the variation of substituents on the phosphorus and α-carbon atoms in the series of transition states **IIc, IVc**–**VIc** (Table 1). The charges on the P^1 and C^3 atoms become positive, and the charge on X^4 only slightly exceeds the charge of the X^4 atom in halophosphorane (for example, Δq(X^4) is –0.14, –0.06, and –0.04 *e* for transition states **Ic**–**IIIc**, respectively), which corresponds, on whole, to sigmatropic pathway *a* of the isomerization reaction in study. The lowest ΔH is characteristic of the fluorotropic transformation, while the chloro- and bromotropism have higher ΔH (see figure).

Table 4. Dependence of the activation energy ($E^{\neq}$, kJ/mol) of the 1,3-halogen shift by sigmatropic pathway *a* and the heats (ΔH^1, kJ/mol) of the imine(phosphorane)–intermediate transformation by dissociation–recombination pathway *b* in the imine–phosphorane system on the degree of solvatation *n* (for solvates M·*n*HCCl$_3$), calculated by the MNDO–PM3 method

Reaction	Mechanism	**Ia**–**Id**, n = 0	**IIa**–**IId**		**IIIa**–**IIId**	
			n = 0	n = 2	n = 0	n = 2
Direct	*a*	173	65	54	43	30
C → P	*b*	325	235	136	219	173
Reverse	*a*	201	115	112	86	78
P → C	*b*	353	285	194	261	220

The effect of substituents on the state of the equilibrium is also clearly pronounced: Electron-acceptor substituents on the phosphorus or nitrogen atoms stabilize the phosphorane [ΔH 49.8 (**IIa, IId**) and 50.3 (**IVa, IVd**) kJ/mol] or imine [ΔH 49.8 (**IIa, IId**) and 37.7 (**VIa, VId**) kJ/mol] isomeric forms, respectively, in complete agreement with the experimental equilibrium constants K_e in methylene chloride: [**VId**]:[**VIa**] = 16:84, [**IIb**]:[**IIa**] = 75:25, and [**IVd**]:[**IVa**] = 100:0 [3]. The 1,3-halogen shift is not accompanied by a noticeable shift of frontier orbitals of the transition state (Table 2). But the highest coefficients on the C^3 and phosphorus atoms and the pyramidalization of these atoms, which favor the strongest overlap of C^3(P) and X^4 orbitals, ensure completion of sigmatropic pathway *a* of the reversible isomerization reaction. The dipole moments of transition states **Ic**–**VIc** span the range 1–4 D, which compares with those of the starting isomers [μ(**Ia**–**VIa**) 3–6 D, μ(**Id**–**VId**) 2–5 D]. Solvation brings the halogen atom X^4 whose tetrahedral environment, along with P and C^3, includes two chloroform molecules, farther apart from the phosphorus atom, and the P^{1}X^{4}C^3 angle slightly

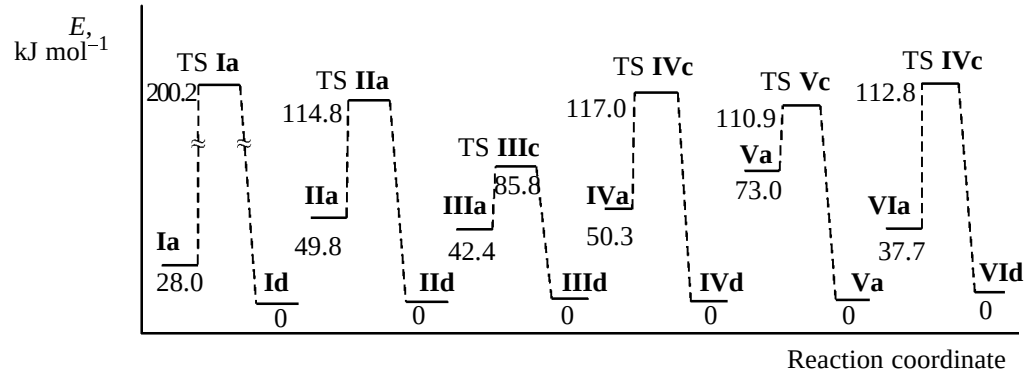

Energy diagrams for the halotropic interconversions of phosphorus imines **Ia**–**VIa** and phosphoranes **Id**–**VId** by sigmatropic mechanism *a*.

decreases (Table 3), which increases the negative charge on X^4 and stabilizes the frontier orbitals (Table 2). The contribution into the localized unshared electron pair of X^4 (localization was performed by Perkins–Stewart [10]) of the orbitals of P^1 and C^3, located in the plane of the $P^1X^4C^3$ triad, slightly decreases. Hence, as the solvation shell is filled, the composition of this orbital changes, for transition states **IIc**, for example, from 85% Cl^4, 12% C^3, and 1% P^1 for $n = 0$ to 86% Cl^4, 12% C^3, and 0% P^1 for $n = 2$, and thus the orbital is stabilized from –12.75 to –13.21 eV. The calculated range of activation energies of the P,C isomerization is 30–201 kJ/mol (see figure), which shows that pathway *a* is feasible only for the chloro- and bromotropism, because the corresponding lower boundary of this range is close to experimental activation barriers (33–77 kJ/mol) for chlorotropism of organophosphorus compounds [11, 12].

Dissociation–recombination pathway *b* of the halotropic isomerization reaction is a two-stage process, in view of the existense of stable intermediates **Ib**–**VIb** whose Hessian is positively determined. Transition states TS1 and TS2 are formed by dissociation of the C^3–X^4 (**Ia**–**VIa**) and P–X^4 (**Id**–**VId**) bonds in the course of formation of intermediates **Ib**–**VIb** (cf. [1]). The halide ion in intermediates **Ib**–**VIb** is located near the *meta* substituent R^3 of the benzene ring at a considerable distance from the exchanging centers but practically in the plane of the PNC^3 triad (Table 1, angle τ). The heat ΔH^1 of the transformation imine(phosphorane) $\rightleftarrows$ intermediate **Ib**–**VIb** in the absence of solvation and with solvation with two chloroform molecules is 2–3 times higher than the activation energy of the 1,3-halotropic shift by pathway *a* (Tables 1, 3, and 4). The activation energy of the rate-limiting stage of pathway *b* would be expected to be even higher, in view of the inequality $E^{\neq}(2) > \Delta H^1(2)$ and with account of the effect of saturation of activation energy with growing solvation shell [1]. Therefore, it becomes evident that the halotropic imine $\rightleftarrows$ phosphorane interconverion may occur in no other way than by sigmatropic mechanism pathway *a*.

REFERENCES

1. Romanenko, E.A., *Teor. Eksp. Khim.*, 1999, vol. 35, no. 4, pp. 215–221.
2. Romanenko, E.A., *Zh. Obshch. Khim.*, 1999, vol. 69, no. 3, pp. 390–399.
3. Boiko, V.I., Samaray, L.I., Mel'nichenko, N.V., Pirozhenko, V.V., Gordeev, A.D., and Soifer, G.B., *Zh. Obshch. Khim.*, 1996, vol. 66, no. 10, pp. 1715–1719.
4. Stewart, J.J.P., *QCPE Program, MOPAC 6.0*, 1990.
5. Gordeev, A.D., Soifer, G.B., Boiko, V.I., and Kozlov, E.S., *Zh. Obshch. Khim.*, 1997, vol. 67, no. 2, p. 516.
6. Romanenko, E.A., Kal'chenko, V.I., and Rudyi, R.B., *Teor. Eksp. Khim.*, 1985, vol. 21, no. 6, pp. 727–730.
7. Holt, E.M. and Holt, S.L., *J. Chem. Soc., Dalton Trans.*, 1974, pp. 1990–1992.
8. Cameron, T.S. and Prout, C.K., *J. Chem. Soc. C*, 1969, pp. 2281–2285.
9. Romanenko, E.A., *Teor. Eksp. Khim.*, 1989, vol. 25, no. 2, pp. 237–240.
10. Perkins, P.G. and Stewart, J.J.P., *J. Chem. Soc., Faraday Trans. 2*, 1982, vol. 78, no. 2, pp. 285–296.
11. Kal'chenko, V.I., Negrebetskii, V.V., Rudyi, R.B., Atomas', L.I., Povolotskii, M.I., and Markovskii, L.N., *Zh. Obshch. Khim.*, 1983, vol. 53, no. 4, pp. 932–934.
12. Kolodyazhnyi, O.I. and Grishkun, V.E., *Heteroatom. Chem.*, 1998, vol. 9, no. 2, pp. 219–228.